

Effects of Annealing and Prior History on Enthalpy Relaxation in Glassy Polymers. 6. Adam–Gibbs Formulation of Nonlinearity

I. M. Hodge

Photographic Research Laboratories, Photographic Products Group, Eastman Kodak Company, Rochester, New York 14650. Received December 4, 1986

ABSTRACT: Alternatives to the Narayanaswamy expression (N) for nonlinearity, $\tau_0 = A \exp[x\Delta h^*/RT + (1-x)\Delta h^*/RT_f]$, were derived from the Adam–Gibbs (AG) theory and fitted to experimental data on five polymers. Two AG-derived expressions were evaluated: $\tau_0 = A \exp[B/RT \ln(T_f/T_2)]$ (“AGL”) and $\tau_0 = A \exp[D/RT(1 - T_2/T_f)]$ (“AGV”). The N and two AG expressions gave comparably good fits for most thermal histories, AGV giving somewhat better fits at the longest annealing times. Reported variations in N parameters with thermal history were shown to be qualitatively consistent with AG predictions. The N parameter, x , was shown to be a direct measure of T_f'/T_2 (T_f' = glassy state value of T_f); the N activation energy, Δh^* , was found to vary inversely with the AG parameters B and D . Correlations of B and D with T_f'/T_2 were observed and shown to be consistent with T_f' approaching T_2 as the AG primary activation energy decreased to zero. The Kohlrausch–Williams–Watt parameter, β , also decreased with decreasing T_f'/T_2 , suggesting increased cooperativity as T_2 is approached. Variations in AG parameters, obtained directly for polymer glasses and indirectly from published N parameters for nonpolymeric glasses, were consistent with generally observed variations in non-Arrhenius behavior above T_g . It was concluded that nonlinear behavior near and below T_g is determined by the same factors that influence equilibrium behavior above T_g .

Introduction

It is well established that relaxation in the glass-transition region and glassy state is nonexponential and nonlinear. Nonexponentiality is demonstrated by the well-known memory effect, in which relaxation from some initial state depends on how that state was reached. This has been discussed in detail by Goldstein¹ and is exemplified by the pioneering experimental studies of borosilicate glass by Ritland² and of poly(vinyl acetate) (PVAc) by Kovacs.³ Nonlinearity is indicated by the asymmetry of relaxation following positive or negative departures from equilibrium. For temperature jumps, nonlinearity is observed for changes greater than about 2 K and gives rise to the characteristically rapid changes in relaxation time during heating through the glass-transition region. Indeed, the term “transition” originates from the sharpness of these changes with temperature. In this paper we formulate the nonlinear aspects of enthalpy relaxation in polymers by extending the Adams–Gibbs theoretical description of linear relaxation processes above T_g .

The most successful method for handling nonlinearity is due to Tool,⁴ who expressed the average relaxation time as a function of the departure from equilibrium. With this approach it is convenient to use the fictive temperature T_f , introduced by Tool and Eichlin⁵ as the “equilibrium temperature” and defined by them as the temperature at which the nonequilibrium value of some macroscopic property would be the equilibrium one. Thus departure from equilibrium is measured by $T_f - T$. This definition of T_f has several limitations, however, that have been discussed in detail by Ritland² and Narayanaswamy.⁶ The most important limitation is the implicit assumption that a single equilibrium state can be associated with every nonequilibrium state, which is valid only for exponential relaxations that exhibit no memory effect. For nonexponential relaxations, the memory effect was interpreted by Narayanaswamy⁶ to mean that some nonequilibrium states comprise several equilibrium states, each with its own fictive temperature. Narayanaswamy handled this intricate problem by assuming a single, thermorheologically simple, nonexponential relaxation mechanism. Changes in actual and fictive temperatures were assumed to shift the time scale only, and for simplicity the shift function was assumed to follow an Arrhenius form

$$\tau_0 = A \exp\left(\frac{H_g}{RT} + \frac{H_s}{RT_f}\right) \quad (1)$$

where A , H_g , and H_s are constant parameters and R is the ideal gas constant. Relaxation can then be described by the usual methods of the linear response theory, modified by eq 1 to include changes in τ_0 as T_f relaxes. In particular, Boltzmann superposition of responses to any thermal history can be applied. This approach to structural relaxation was pioneered by Mazurin, Rekhson, and Startsev.⁷ Moynihan et al.⁸ rewrote eq 1 as

$$\tau_0 = A \exp\left[\frac{x\Delta h^*}{RT} + \frac{(1-x)\Delta h^*}{RT_f}\right] \quad (2)$$

where $1 \geq x > 0$, and it is in this form that the Narayanaswamy (N) expression is usually used. For nonpolymeric materials the parameter Δh^* usually equals the readily evaluated activation energy for shear viscosity above T_g . For polymers, however, entanglements determine the viscosity in the terminal region and other methods must be used. The method of choice is to determine the cooling-rate dependence of the glassy-state value of T_f , T_f' ,⁸ obtained by integration of the normalized heat capacity measured on heating.

Although the N expression describes the glass transition and glassy-state relaxations very well, it has several shortcomings. As noted earlier,⁹ these include the following:

1. The prediction of an Arrhenius temperature dependence for the equilibrium state ($T_f = T$), in conflict with the well-established Vogel¹⁰ and WLF¹¹ expressions. Associated with this are unusually large values of $\Delta h^*/R$, as high as 225 kK.^{12,13}
2. The expression is empirical, and the parameters x and Δh^* have no clear physical interpretation.
3. The physical origin of the inverse correlation between x and Δh^* ¹³ is obscure.
4. Systematic changes in N parameters with thermal history, particularly in x , have been reported by several groups.^{14–16} These appear to be more pronounced at long annealing times and low annealing temperatures. It has been suggested by Chen and Kurkjian¹⁷ that these indicate a qualitative distinction between glassy-state relaxations

and the glass transition. An alternative view^{14,15} is that the problem resides in the N expression for the partitioning of T and T_f . It is our opinion that the correct formalism for the glass-transition kinetics has yet to be found and that the N expression for nonlinearity is indeed suspect.

In seeking a theoretical basis for nonlinearity it is natural to consider free-volume theories. However, although free volume, V_f , can be associated with a fictive temperature, there is no direct method for introducing the actual temperature. Macedo and Litovitz¹⁸ have criticized the usual free-volume derivations for neglecting the thermal activation needed for a particle to move from one pocket of free volume to another and derived the hybrid expression

$$\tau_0 = A \exp(B/V_f + E/RT) \quad (3)$$

where A , B , and E are constant parameters. Putting $V_f \sim T_f - T_2$, where T_2 is the temperature of zero free volume, yields

$$\tau_0 = A \exp[B'/R(T_f - T_2) + E/RT] \quad (4)$$

whose linear form ($T_f = T$) was first proposed by Dienes.¹⁹ Equation 4 correctly predicts an Arrhenius temperature dependence in the glassy state but does not produce the Vogel form at equilibrium. Nevertheless, the Dienes equation was found by Macedo and Litovitz to give a good account of the viscosity of B_2O_3 , SiO_2 , alkali silicates, alcohols, and poly(isobutylene). Note that B' and E in eq 4 are independent quantities, related to free-volume fluctuations and thermal activation barriers, respectively, so that eq 4 has the disadvantage of having an additional independent parameter compared with N.

Mazurin et al.²⁰ proposed the equation

$$\tau_0 = A \exp[Q_1/R(T_f - T_2) + (Q_2/R)(T^{-1} - T_f^{-1})] \quad (5)$$

where A , Q_1 , Q_2 , and T_2 are constant parameters. This is similar to eq 4 but produces the Vogel form in the equilibrium state. However, it shares with N the disadvantage of being empirical and like eq 4 has an additional independent parameter.

Entropy-based theories offer a more promising approach because they produce a natural separation of actual and fictive temperatures. The Adam-Gibbs theory²¹ (AG) is the most familiar of these and provides the foundation for our treatment of nonlinearity. The AG expression for relaxation time τ_0 is

$$\tau_0 = A \exp\left(\frac{\Delta\mu s_c^*}{RTS_c}\right) \quad (6)$$

where A is a constant, $\Delta\mu$ is the free-energy barrier hindering rearrangement, s_c^* is the configurational entropy of the smallest group able to rearrange, and S_c is the macroscopic configurational entropy. The fictive temperature is introduced into the expression for S_c as

$$S_c = \int_{T_2}^{T_f} \Delta C_p/T \, dT \quad (7)$$

where ΔC_p is the configurational heat capacity and T_2 is the configurational ground-state temperature, conceptually identical with T_2 in the Gibbs-DiMarzio²² thermodynamic theory of the glass transition. Equation 7 expresses the idea that the fictive temperature of a glass is a measure of its configurational entropy and that loss of excess entropy during annealing corresponds to relaxation of T_f toward the annealing temperature, T_e . In applying the AG expression to enthalpy relaxation, it must be assumed that the entropic and enthalpic fictive temperatures are the same. This is a good approximation, however, because the range in T and T_f for the glass-transition and annealing

processes is sufficiently narrow that the integrals of ΔC_p and $\Delta C_p/T$ are nearly proportional. For example, a range of 20 K produces a difference in entropic and enthalpic T_f on the order of 0.1 K.

Explicit expressions for $\tau_0(T, T_f)$ derived from eq 6 and 7 depend on the temperature dependence of ΔC_p . For constant ΔC_p ,

$$\tau_0 = A \exp[B/RT \ln(T_f/T_2)] \quad (8a)$$

where

$$B = \Delta\mu s_c^*/\Delta C_p \quad (8b)$$

Plazek and Magill²³ observed that the experimental ratio of activation energies for creep recovery in 1,3,5-tri- α -naphthylbenzene, above and below T_g , was in excellent agreement with eq 8 with parameters determined above T_g . Magill²⁴ also found that $\log(\text{viscosity})$ varied linearly with $(TS_c)^{-1}$ at low temperatures near T_g , in accordance with eq 6, but failed at high temperatures where the AG assumptions were probably inapplicable.

Approximate relations between the parameters of eq 2 and 8 can be derived from appropriate temperature derivatives ($T_f = \text{unannealed glassy state value of } T_f$):

$$\Delta h^*/R = \frac{d \ln \tau_0}{d(1/T)} \approx B(L^{-1} + L^{-2}) \quad (9a)$$

where

$$L \equiv \ln(T_f'/T_2) \quad (9b)$$

and

$$x \Delta h^*/R = \left. \frac{\partial \ln \tau_0}{\partial(1/T)} \right|_{T_f} \approx B/L \quad (10)$$

from which

$$x \approx L/(1 + L) \quad (11)$$

Equations 9 and 10 were first derived by Plazek and Magill,²³ using a different notation. Because of the logarithmic term in T_f , we refer to eq 8 as AGL.

For ΔC_p with the temperature dependence

$$\Delta C_p = CT_g/T \quad (12)$$

where $C = \Delta C_p$ at T_g , it has been shown^{9,25} that

$$\tau_0 = A \exp[D/RT(1 - T_2/T_f)] \quad (13)$$

from which

$$\Delta h^*/R \approx D/(1 - T_2/T_f)^2 \quad (14)$$

and

$$x \approx 1 - T_2/T_f' \quad (15)$$

where $D = \Delta\mu s_c^* T_2/CT_g$. In the equilibrium state eq 13 assumes the Vogel form

$$\tau_0 = A \exp[D/R(T - T_2)] \quad (16)$$

and we therefore refer to eq 13 as the Adam-Gibbs-Vogel (AGV) equation. Equation 12 is the simplest expression of the experimental observation that ΔC_p decreases with increasing temperature, although it is recognized that the empirical form

$$\Delta C_p = a - bT \quad (17)$$

is generally more accurate.

The AG equation was also discussed by Howell et al.²⁶ in their study of the molten salt $0.4Ca(NO_3)_2 \cdot 0.6KNO_3$. They derived the following general expressions for the effective activation energies above and below T_g :

$$\Delta h^* = E/S_c(T) + [ET/S_c^2(T)] \frac{dS_c(T)}{dT} \quad (18)$$

$$x\Delta h^* = E/S_c(T_f') \quad (19)$$

where $E = \Delta u_{s_c}^*$. These investigators observed that S_c must always decrease with decreasing T_f ($\Delta C_p > 0$), and the value of $x\Delta h^*$ must therefore increase with decreasing T_f . In this respect both the AGL and AGV equations differ significantly from the empirical eq 4 and 5, both of which predict an Arrhenius activation energy in the glassy state that is independent of T_f' . Matsuoka²⁷ has shown that for dielectric and mechanical relaxation in PVAc the parameter E in eq 4 varies with T_f' in a manner consistent with the AG theory.

The AG expression was first applied to structural relaxation by Scherer²⁸ in his analysis of NBS-710 soda-lime-silicate glass. He inserted eq 17 into eq 7, using calorimetrically measured values for the coefficients a and b , and obtained an excellent description of published viscosity,²⁹ refractive index,³⁰ and enthalpy³¹ data.

We conclude this Introduction with a few brief comments on the parameter T_2 , which appears in the AGL, AGV, and other expressions for $\tau_0(T, T_f')$. The concept of a thermodynamically defined glass temperature T_2 originated with Kauzmann.³² For many inorganic and some polymeric materials, T_2 can be calculated from the (temperature-dependent) difference in heat capacity of the liquid and crystal (\approx glass), ΔC_p , the enthalpy of melting, ΔH_m , and the melting temperature, T_m :

$$\Delta H_m/T_m = \int_{T_2}^{T_m} \Delta C_p/T \, dT \quad (20)$$

It is assumed in this analysis that ΔC_p equals the configurational heat capacity, although this has been challenged by Goldstein,³³ who pointed out that ΔC_p can contain large vibrational and other contributions. For inorganics the calculation of T_2 from eq 20 is usually unambiguous, although care must be taken to properly include the entropy of solid-state transitions in some cases. For polymers, however, crystallizable forms usually have different tacticities from purely amorphous forms, and it must be assumed that ΔC_p , ΔH_m , and T_m do not change with tacticity, or change in a known way. It has also been argued³⁴ that the Kauzmann estimate of T_2 for polymers is an artifact of incorrect extrapolation of $\Delta C_p(T)$ below T_g , and the Gibbs-DiMarzio theory²² has also been criticized.³⁵ Here, we assume that a configurational ground state for the amorphous state is conceptually possible, and that T_2 is physically relevant to relaxation behavior.

Calculation and Fitting Procedures

The method for calculating normalized heat capacities C_p^N was similar to that described previously.¹² Nonexponentiality is described by the celebrated Kohlrausch-Williams-Watt function

$$\phi(t) = \exp[-(t/\tau_0)^\beta] \quad 1 \geq \beta > 0 \quad (21)$$

with τ_0 expressed as a function of T and T_f' according to the AGL or AGV expressions. Equation 21 was first applied to structural relaxation by Rekhson et al.³⁶ and is known to be quite accurate for a large number of relaxation processes in condensed media. The methods for dividing the annealing time, t_e , into subintervals, and for calculating high-heat-capacity overshoots, differed somewhat from earlier studies, however. First, t_e was divided into five subintervals per decade of time (in seconds), rather than a constant total of 10 subintervals. This produced more accurate values of T_f' for long t_e . Second, for large over-

Table I
Narayanaswamy Parameters

material	ln A, s	$\Delta h^*/R$, kK	x	β	ref
PVAc	-224.5	71	0.35	0.57	38
	-277.50	88	0.27	0.51	this work
PVC	-622.0	225	0.10	0.23	this work
PS	-211.20	80	0.49	0.74	this work
PMMA	-357.8	138	0.19	0.35	this work
PC	-355.8	150	0.19	0.46	this work
As ₂ Se ₃	-85.5	40.9	0.49	0.67	39
B ₂ O ₃	-75.6	45	0.40	0.65	40
5P4E	-153.1	38.5	0.40	0.70	39
Ca ²⁺ -K ⁺ -NO ₃ ⁻	-202.47	70	0.31	0.46	41
NaKSi ₃ O ₇	-62.79	49	0.70	0.66	42
ZBLA ^a	-282.6	165	0.19	0.50	43

^a See ref 43 for explicit composition. Δh^* taken from ref 43.

shoots the usual constant-temperature step, ΔT_j , of 1 K was reduced in inverse proportion to C_p^N calculated for the previous step, $C_{p,j-1}^N$:

$$\begin{aligned} \Delta T_j &= 1/C_{p,j-1}^N \quad C_{p,j-1}^N > 1 \\ &= 1.0 \quad C_{p,j-1}^N \leq 1 \end{aligned} \quad (22)$$

This procedure ensured that changes in T_f did not exceed 2 K per step, for C_p^N overshoots less than about 5 or 6. For higher overshoots, this procedure did not guarantee that $\Delta T_f < 2$ but was tolerated since only one set of data exhibited an overshoot of more than 6. The new procedure also generated values of C_p^N at noninteger temperatures; values at integer temperatures, needed to fit experimental data, were obtained by linear interpolation. The Marquardt algorithm for obtaining best-fit parameters was described earlier.³⁷ As before,^{13,37} one of the four parameters was fixed and the other three optimized. Initial studies indicated that fixing B (AGL) or D (AGV), eq 8 and 13, produced values of T_2 , A , and β that depended on their starting values. Better behavior was found when T_2 was fixed. In this case starting values of B and D were calculated from T_2 and experimental values of T_f' and Δh^* , using eq 9 and 14. Starting values for ln A were calculated by placing $\tau_0 = 10$ s at $T = T_f = T_f'$ into the appropriate equation for τ_0 , and starting values β were set equal to published N values.¹³ Averaged sets of parameters were obtained for values of T_2 that gave the lowest overall residuals. Because the calculation procedure differed from earlier versions, new sets of N parameters were also obtained, with Δh^* fixed at the experimental values^{12,13,37} determined from the cooling-rate dependence of T_f' .⁸

Results

The new N parameters for polystyrene PS, PVAc, poly(methyl methacrylate) (PMMA), and bisphenol A polycarbonate (PC) are collected in Table I, together with those obtained by others for nonpolymeric glasses. An additional set of parameters was obtained for PVAc with $\Delta h^*/R = 71$ kK, the activation energy reported by Sasabe and Moynihan.³⁸

Best-fit AGL and AGV parameters for polymers, and those for nonpolymeric glasses estimated from published N parameters, are given in Tables II and III, respectively. Two sets of AGV parameters are given for PS (see Discussion). Experimental and calculated values of $C_{p,\max}^N$ and T_{\max} for poly(vinyl chloride) PVC are given in Table IV as a function of T_e and t_e (here $C_{p,\max}^N$ is the maximum value of C_p^N for the annealing-induced endotherm and T_{\max} the temperature at which it occurs).

AGV fits for PS are shown in Figures 1-3, for PVAc in Figures 4 and 5, for PMMA in Figures 6 and 7, and for PC in Figures 8 and 9. The AGL and new N parameters gave similar fits in most cases and are compared with AGV fits

Table II
Summary of AGL Parameters

material	ln A, s	B/R, kK	T ₂ , K	β	Δh* _{eff} /R (at T' _f)	Δh* _{eff} /R (at T _{max})	x _{eff} (at T' _f)
PVAc	-69.00	7.55	225	0.54	95	84	0.25
PVC	-60.00	2.81	320	0.27	226	153	0.10
PS	-91.00	25.9	180	0.71	84	81	0.42
PMMA	-53.46	3.57	325	0.33	171	127	0.14
PC	-78.00	14.4	275	0.60	117	109	0.30
As ₂ Se ₃ ^a	-43.0	19.2	178	0.67			
B ₂ O ₃ ^a	-32.0	12.0	287	0.65			
5P4 ^a	-63.0	10.27	126	0.70			
Ca ²⁺ -K ⁺ -NO ₃ ^{-a}	-62.8	9.75	220	0.46			
NaKSi ₃ O ₇ ^a	-17.4	30.0	72	0.66			
ZBLA ^a	-58.0	7.35	476	0.50			

^a Obtained from N parameters by using eq 9-11.

Table III
Summary of AGV Parameters

material	ln A, s	D/R, kK	T ₂ , K	β	Δh* _{eff} /R (at T' _f)	Δh* _{eff} /R (at T _{max})	x _{eff} (at T' _f)
PVAc	-66.60	6.23	225	0.55	82	72	0.28
PVC	-59.74	2.61	320	0.28	211	130	0.11
PS	-100.30	17.1	210	0.74	90	85	0.44
	-63.50	7.63	260	0.54	83	80	0.30
PMMA	-55.45	3.43	325	0.34	166	123	0.14
PC	-70.30	7.03	325	0.54	144	127	0.22
As ₂ Se ₃ ^a	-43.1	9.82	237				
B ₂ O ₃ ^a	-26.1	7.20	336				
5P4E ^a	-63.0	6.16	147				
Ca ²⁺ -K ⁺ -NO ₃ ^{-a}	-62.9	6.73	238				
NaKSi ₃ O ₇ ^a	-46.3	24.0	222				
ZBLA ^a	-53.0	5.96	525				

^a Obtained from N parameters by using eq 14 and 15.

Table IV
N, AGL, and AGF Calculated Values of C_{p,max}^N and T_{max} for PVC

T _e , K	t _e , h	C _{p,max} ^N				T _{max} , K			
		obsd ^a	N	AGL	AGV	obsd ^a	N	AGL	AGV
293	7	0.13	0.03	0.06	0.06	324	306	318	318
	27	0.14	0.04	0.09	0.09	328	310	322	322
	150	0.21	0.07	0.15	0.15	332	317	328	328
313	6	0.16	0.20	0.20	0.20	336	337	337	337
	24	0.33	0.31	0.31	0.31	341	341	341	341
	50	0.40	0.39	0.39	0.39	343	343	343	343
333	1	0.21	0.36	0.39	0.40	351	349	350	350
	7	0.66	0.66	0.79	0.80	357	354	354	354
	24	1.10	1.05	1.2	1.2	359	356	357	357
	50	1.60	1.4	1.7	1.8	360	358	358	358

^a Reference 12.

to selected thermal histories for each polymer in Figure 10. Experimental and calculated values of T'_f for PS at the start of reheating are plotted as a function of t_e and T_e in Figure 11. Plots of T'_f as a function of t_e only are given in Figure 12 for PMMA and PC.

Discussion

The new N parameters are very similar to those reported previously,^{12,13,37} indicating that the modified calculation procedure has only minor effects for most polymers (except PS and PVC, see below). The x and β parameters for PVAc for Δh*/R = 71 kK are in broad agreement with those reported by Sasabe and Moynihan³⁸ for the same value of Δh*/R. The differences (0.06 in each) are close to experimental uncertainty, but to the extent they are significant can probably be attributed to sample differences. The N parameters for PS are also in good agreement with those reported by Privalko et al.⁴⁴ for monodisperse, low molecular weight PS (M_n ≈ 9-17 × 10³). The x parameter for ZBLA glass is in exact agreement with an approximate estimate.⁴³ However, there is a large dis-

crepancy between the N parameters for atactic PMMA found here and those reported by Tribone et al.,¹⁵ although the β parameters are in agreement. The differences in Δh*, and probably x, are almost certainly due to the different methods used to define Δh* (cooling-rate dependence of T'_f for the present work and heating-rate dependence of T_g at constant cooling rate = 20 K min⁻¹ by Tribone et al., where T_g was determined from the extrapolated gradient near C_p^N = 0.5). Calculations of the heating-rate dependence of T_g at QC = 20 K min⁻¹, using the N parameters for PMMA obtained here, produced a value for d ln QH/R d(1/T_g) of about 100 ± 20 kK, in agreement with 105 kK quoted by Tribone et al. for atactic PMMA. Thus the two sets of data may not be inconsistent.

These calculations also demonstrate quite clearly that activation energies obtained from the heating-rate dependence of T_g at constant cooling rate do not necessarily correspond to Δh* in the N expression for τ₀. On the other hand, the cooling-rate dependence of T'_f gives the correct Δh*,⁸ and also has distinct experimental advantages. First, temperature calibration need not be applied to cooling

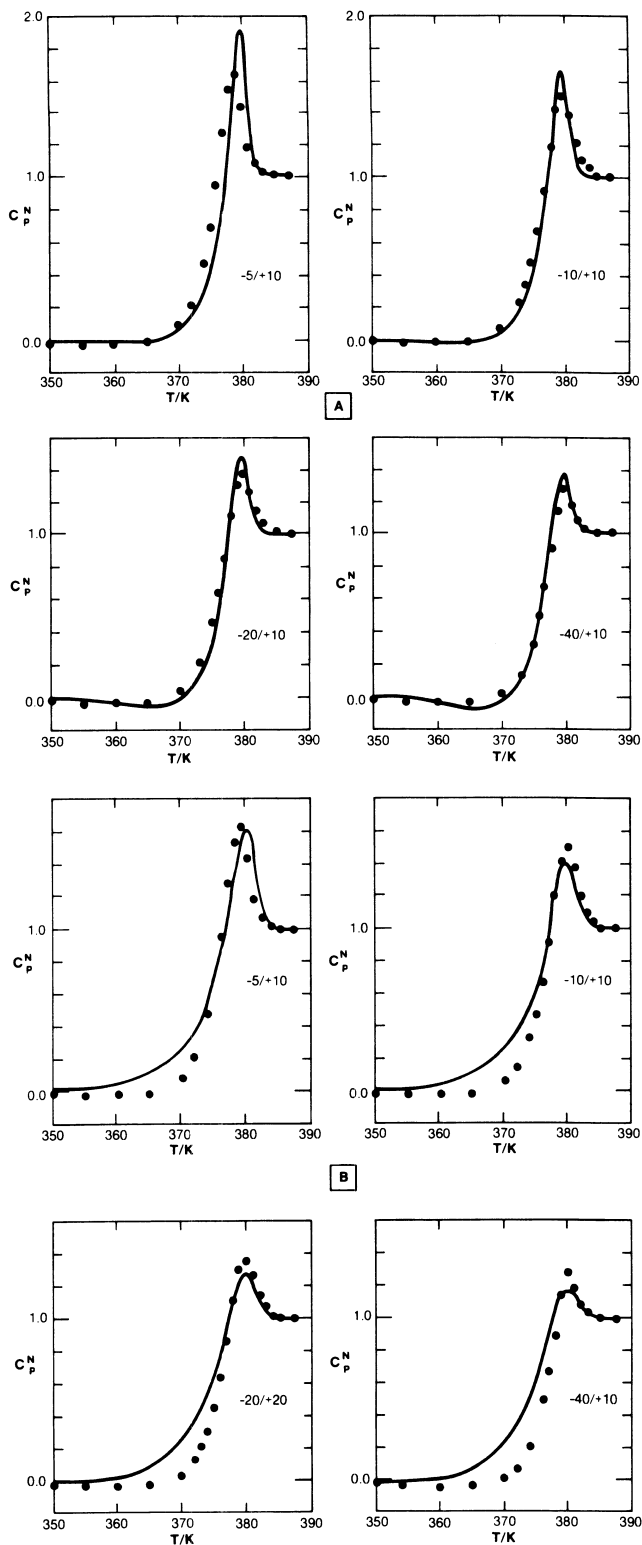


Figure 1. AGV fits (lines) to PS data (points) for indicated cooling and heating rates $-QC/+QH$, without annealing. (A) Parameters for $T_e = 210$ K (Table III). (B) Parameters for $T_e = 260$ K (Table III).

since T_f' is determined from integration of the heating curve,⁸ it is sufficient that the cooling rate be known. Second, temperature calibration is needed for a single heating rate only. In fact, it need not be applied at all for obtaining Δh^* if the temperature correction δT is constant and small, since the error produced by measuring $d \ln QC/d(T_f' + \delta T)^{-1}$ rather than $d \ln QC/d(1/T_f')$ is also small (a few percent for $\delta T = 5$ K at $T_f' \approx 300$ K, for example). Third, integration of $C_p^N(T)$ to obtain T_f' eliminates

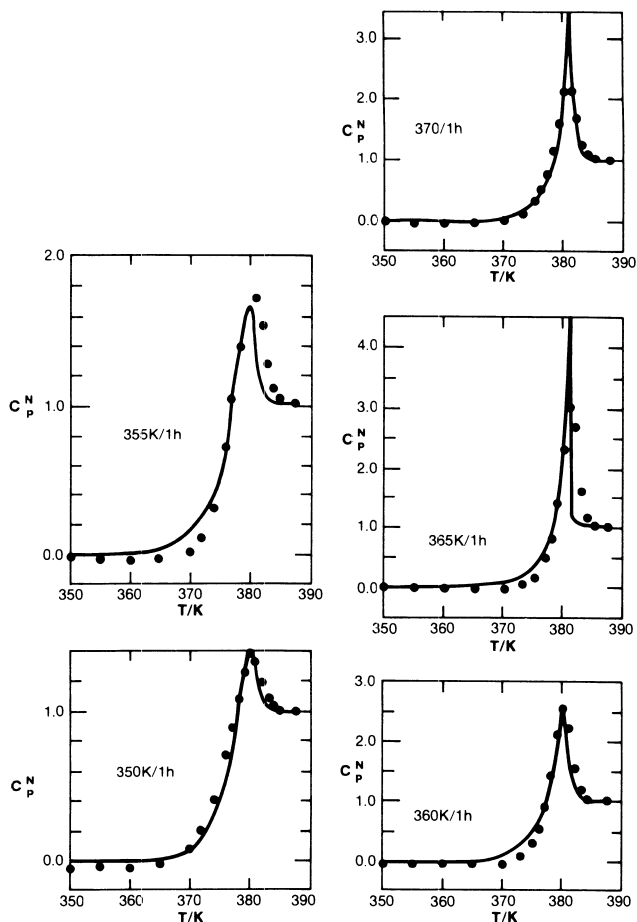


Figure 2. AGV fits (lines) to PS data (points), as a function of T_e for $t_e = 1$ h. Parameters for $T_2 = 210$ K (Table III). Cooling rate = 40 K min^{-1} ; heating rate = 10 K min^{-1} .

thermal lag effects since these affect only the shape of $C_p^N(T)$.

The fits provided by the N, AGL, and AGV formalisms are comparably good for the limited range of thermal histories studied here (Figure 10). For PMMA and PC all three formalisms also give approximately equivalent descriptions of T_f' as a function of T_e for $t_e = 1$ h (Figure 12). For PS, on the other hand, the AGV formalism gives a better account of T_f' as a function of t_e (Figure 11), and it appears that AGV may give increasingly better fits to T_f' for longer t_e . This possibility is confirmed for PVC (Table IV), where the long t_e and low T_e data are reproduced significantly better by AGV compared with N. The AGV expression is also marginally better than N for describing low-temperature anneals of B_2O_3 . Chen and Kurkjian¹⁷ observed a broad sub- T_g endotherm of normalized magnitude 0.05 centered near 510 K, following annealing at $T_e = 420$ K $\approx T_g - 160$ K for $t_e = 30$ h (QC = 80 K min^{-1} , QH = 20 K min^{-1}). The N parameters obtained by Moynihan et al.⁴⁰ predict 0.02 at about 500 K for this history, compared with 0.03 near 510 K predicted by the N-derived AGV parameters. Both formalisms correctly reproduce the normalized overshoot at T_g , 1.28 (1.30 for N, 1.27 for AGV). For $\beta = 0.60$ rather than 0.65 (the lower limit of uncertainty), the AGV formalism predicts a broad endotherm of 0.05 around 520 K, in agreement with experiment, compared with 0.04 near 510 K predicted by N. These results also suggest that a separate relaxation mechanism need not be invoked to account for the small annealing endotherms in this material.

The most commonly observed systematic change in N parameters with thermal history is an increase in x with

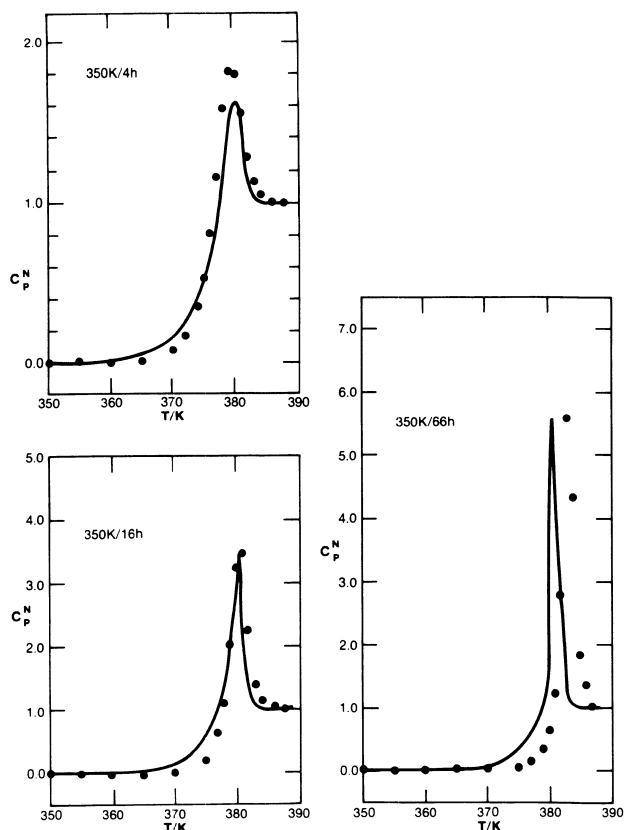


Figure 3. Like Figure 2, but as a function of t_e at $T_e = 350$ K.

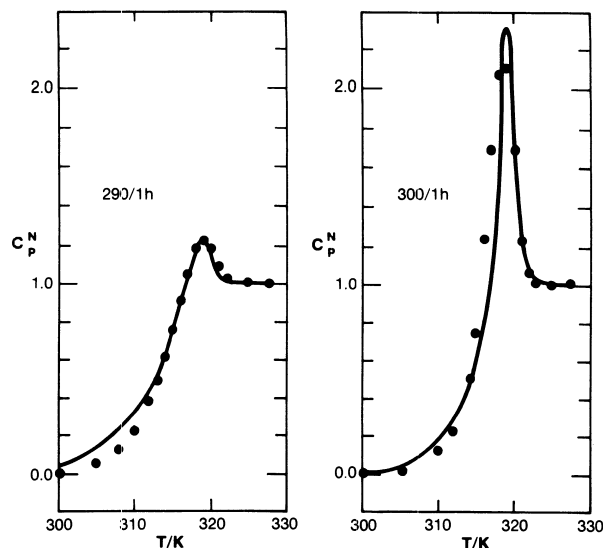


Figure 5. AGV fits to PVAc data for 1 h anneals at 290 and 300 K. Parameters given in Table III.

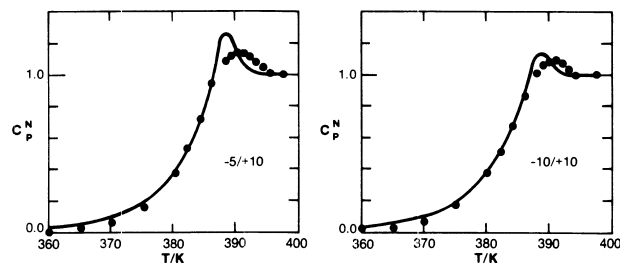


Figure 6. AGV fits to PMMA data for the indicated cooling and heating rates $-QC/+QH$. Parameters given in Table III.

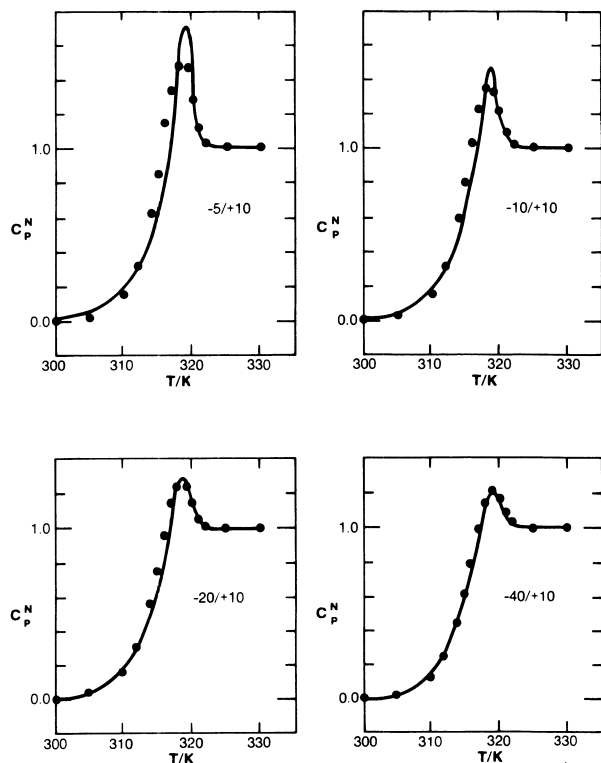


Figure 4. AGV fits (lines) to PVAc data (points) for the indicated cooling and heating rate $-QC/+QH$. Parameters given in Table III.

increasing t_e and higher T_e .^{14,15} Both effects correspond to x increasing with decreasing T_f' , in apparent conflict with the AGV prediction (ref 14 and Table VI for PS in this paper). This may be due in part to $x\Delta h^*$ increasing at constant Δh^* , but the matter is more complex. To study this, a single set of AGV parameters was used to generate C_p^N data for several thermal histories and best-fit N pa-

rameters obtained for each (Table VII). Both x and β increased with t_e and T_e , as observed experimentally. Inspection of the best-fit N and "averaged N" predictions revealed that the systematic changes in best-fit N parameters were being forced by the magnitude of the normalized overshoot, $C_{p,max}^N$, rather than the value of T_f' after annealing. The AGV function produces smaller overshoots, because of greater self-retardation and smaller changes in T_f' during annealing and because the value of x_{eff} is greater near T_{max} and relaxation therefore less accelerating through the overshoot region. To reduce $C_{p,max}^N$ the N optimization evidently increases x both to produce lower values of T_f' at the start of aging, and therefore decrease the rate of annealing despite less retarding kinetics, and to reduce acceleration during heating through the overshoot region. The parameter β evidently changes with thermal history because it also influences the overshoot. The absence of changes in β observed by Tribone et al.¹⁵ may be due partly to their different definition of Δh^* (see above) and partly to their use of a different (better?) optimization algorithm.

These results emphasize the importance of accurate data in the overshoot region and raise the issue of thermal lag

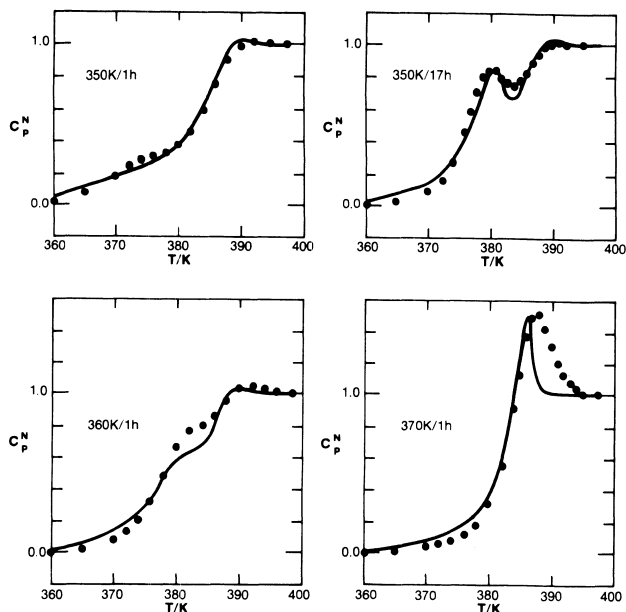


Figure 7. AGV fits to PMMA data for the indicated combinations of T_e/t_e . Cooling rate = 40 K min^{-1} ; heating rate = 10 K min^{-1} . Parameters given in Table III.

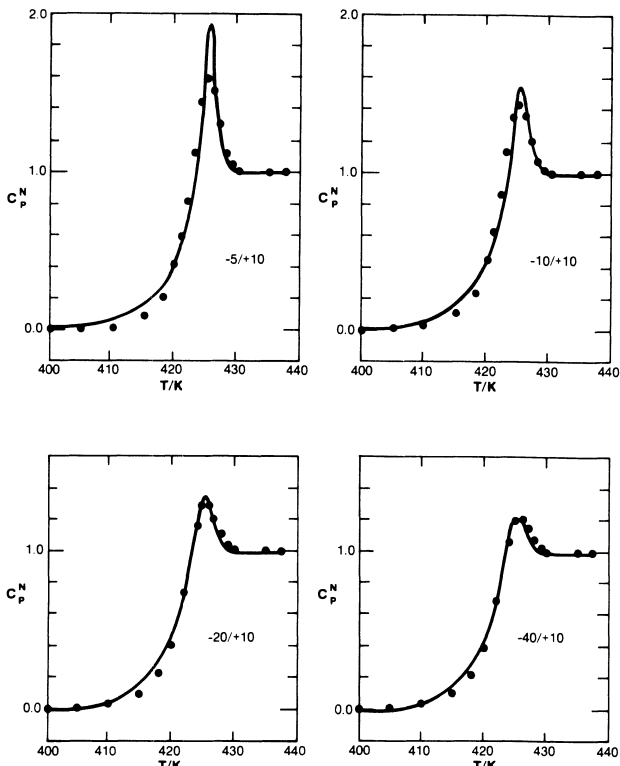


Figure 8. AGV fits to PC data for the indicated cooling and heating rates -QC/+QH. Parameters given in Table III.

effects. DeBolt³⁰ measured temperature differences of the order of 1 K in DSC samples that increased with heating rate, and these are presumably also affected by sample morphology and thermal contact with the sample pan. Since experimentally observed overshoots for polymers are frequently quite high and sharp, with widths at half-height of the order of 2 or 3 K, temperature gradients of 1 K or so in the sample are expected to be significant. To assess temperature-gradient effects, calculated heat capacity curves were displaced by up to ± 1 K at 0.01 K intervals and averaged. A typical result was a reduction in overshoot from 8.6 with no gradients, to 6.9 for a temperature range of 1 K, to 5.3 for a range of 2 K. Thus parameters obtained

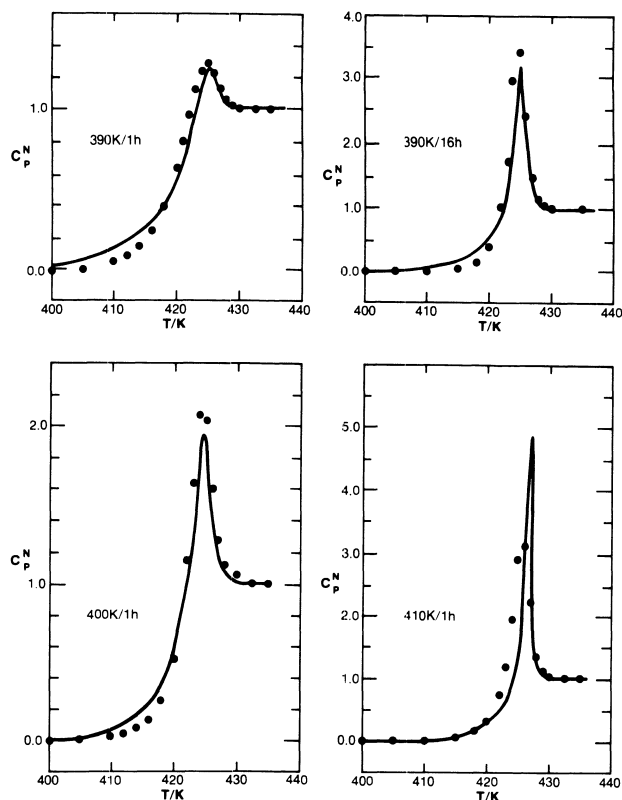


Figure 9. AGV fits to PC data for the indicated combinations of T_e/t_e . Cooling rate = 40 K min^{-1} ; heating rate = 10 K min^{-1} . Parameters given in Table III.

from high overshoot data may be incorrect, and better methods are needed for comparing the merits of the N and AG formalisms at long annealing times. A good alternative in our view is to obtain best-fit parameters from low overshoot data and test their predictions of T_f' at long annealing times, since the area under $C_p^N(T)$ is not influenced by thermal lag.

Because the best-fit AGL and AGV parameters are determined to a large extent by data near $C_{p,\text{max}}^N$, the values of Δh^*_{eff} are determined by T_{max} rather than T_f' . Since T_{max} is typically 10 K or so higher than T_f' , Δh^*_{eff} at T_{max} should be lower than the experimental values obtained from the cooling-rate dependence of T_f' . This is found, but the differences are generally within estimated experimental uncertainties (Tables II, III). However, a definite difference is observed for PVC, and for N fits to the AGV-generated data discussed above. In the last case, a value for $\Delta h^*/R$ of 90 kK is found from the cooling-rate dependence of T_f' , compared with the best-fit value of 80 kK (see Table VII). These small effects notwithstanding, the generally good agreement between x_{eff} and Δh^*_{eff} calculated from the AGL and AGV parameters and the best-fit N values indicates that eq 9, 11, 14, and 15 are good approximations. This agreement also suggests that experimental heat capacity data contain enough information to give accurate best-fit values of Δh^* . This is perhaps surprising but is confirmed by the observation that AGL and AGV parameters for different values of T_2 produce similar values of Δh^*_{eff} , as a result of compensating changes in B or D (e.g., compare Δh^*_{eff} for $T_2 = 210$ and 260 K for PS, Table III). This is probably due, at least in part, to Δh^* determining the temperature range of the glass transition and thus the area under $C_p^N(T)$, almost independent of T_2 or x .

The variations in $\ln A$ for AGL and AGV fits to the polymers are considerably smaller than those for N. Standard deviations for both AG forms are about 25% of

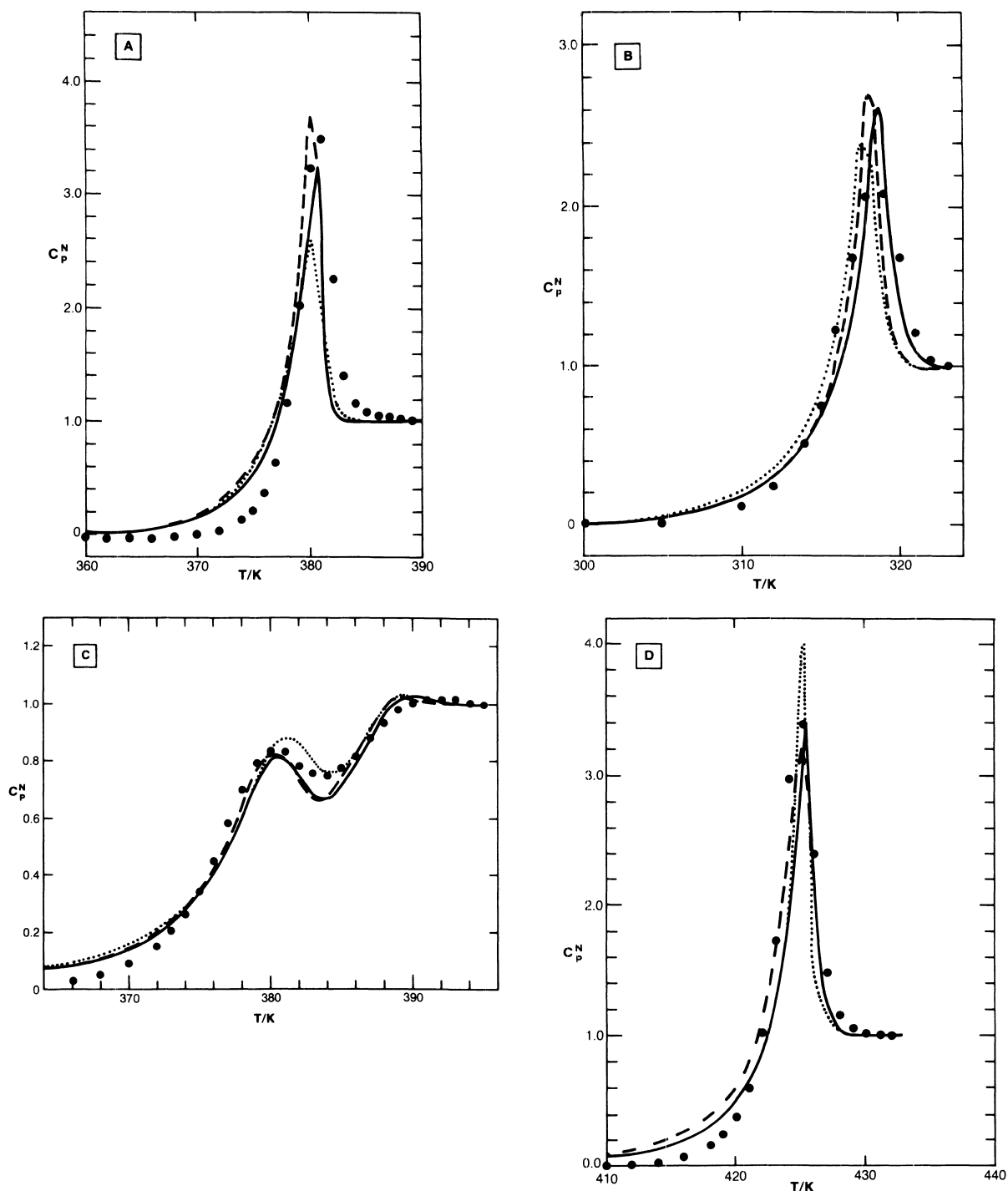


Figure 10. Comparison of N (---), AGL (---), and AGV (—) fits, parameters given in Tables I–III. (A) PS data for $t_e = 16$ h at $T_e = 350$ K. AGV parameters for $T_2 = 210$ K. (B) PVAc data for $t_e = 1$ h at $T_e = 300$ K. N parameters for $\Delta h^*/R = 88$ kK. (C) PMMA data for $t_e = 17$ h at 350 K. (D) PC data for $t_e = 16$ h at $T_e = 390$ K.

the mean, compared with 40% for N, and these are reduced to 10% if the value for PS is omitted or the value for $T_2 = 260$ K is included in the AGV average. Although theoretical accounts of preexponential factors are not well developed in general, the smaller variation in $\ln A$ for the AG fits suggests that AG is a more consistent description. However, the magnitudes of A , about $10^{-26 \pm 2}$ s, remain problematic. The theory of Ngai and co-workers^{45,46} can account for this result for $\beta = 0.25$ but appears to fail at larger values of β .

Uncertainties in the best-fit values of T_2 are particularly large, because variations in T_2 can be compensated for by changes in B or D to produce similar values of Δh^*_{eff} . We estimate ± 15 K for PVC, ± 30 K for PVAc, PMMA, and

PC, and ± 40 K for PS (corresponding roughly to 10% uncertainties in the N parameter x). Kauzmann evaluations of T_2 for most polymers are also very uncertain, as discussed in the Introduction. However, good Kauzmann estimates of T_2 are available for PS: 280 ± 15 K by Karasz et al.⁴⁷ and 260 ± 15 K by Miller.⁴⁸ The best-fit AGV value of 210 K is lower than both of these, although the upper limit of the estimated AGV uncertainty range overlaps with the lower limit of Miller's range. In view of the large uncertainties in T_2 , an additional set of AGV parameters for $T_2 = 260$ K was determined (Table III). The corresponding fits for simple thermal histories (no annealing) are shown in Figure 1B, and are much broader than the data. The fits to thermal histories with annealing are

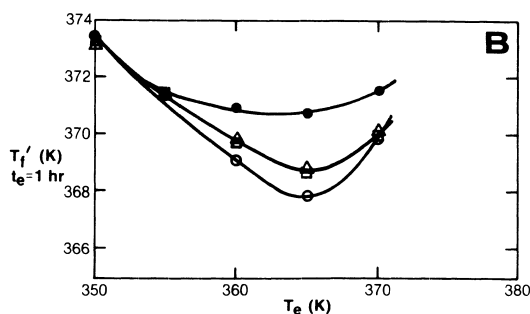
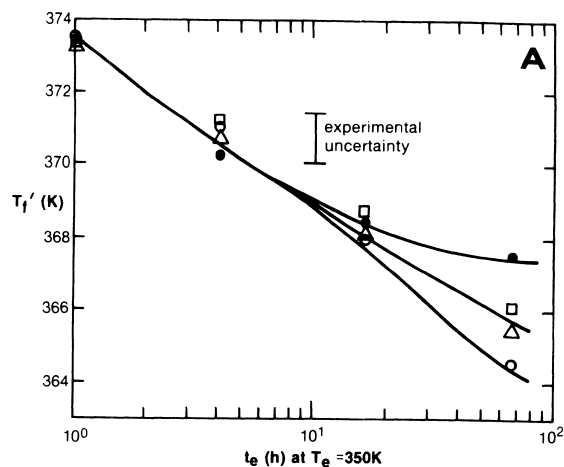


Figure 11. (A) N (○), AGL (△), and AGV (□) fits to T_f' data (●) as a function of t_e at $T_e = 350$ K for PS. Parameters as in Figure 2. (B) N, AGL, and AGV fits to T_f' as a function of T_e for $t_e = 1$ h, for PS. Parameters as in Figure 2.

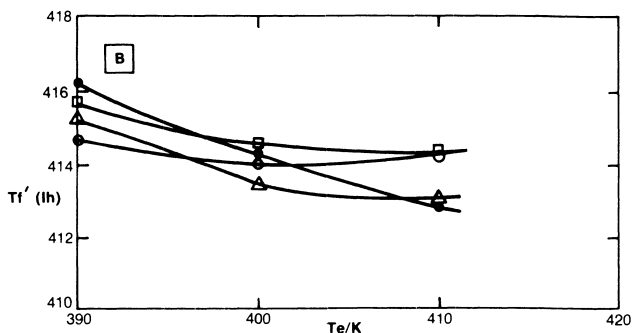
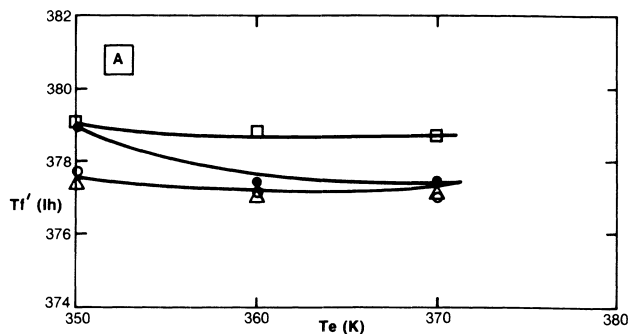


Figure 12. (A) N (○), AGL (△), and AGV (□) fits to T_f' data (●) as a function of T_e for $t_e = 1$ h, for PMMA. Parameters given in Tables I-III. (B) Same fits for PC.

similar. However, these parameters produce a small shoulder below T_g for the annealing history studied by Chen and Wang⁴⁹ for a monodisperse PS (260 h at 320 K), which is similar to but smaller than the experimentally

Table V
Estimates of $\Delta\mu$ from AGV Parameters

polymer	D/R , kK	ΔC_p^a , J mol ⁻¹ K ⁻¹	no. of beads	$\Delta\mu/k$, kK for $s_c^* =$	
				$k \ln 2$	$k \ln 3!$
PVAc	6.23	35	4	6.8	2.6
PVC	2.61	18	2	3.6	1.4
PS	17.1	33	3	18	7.0
PMMA	3.43	30	3	4.9	1.9
PC	3.43	30	4	3.7	1.4
	7.03	62	5	9.8	4.6
	7.03	62	6	12	3.8

^aFrom tabulation in ref 52.

observed shoulder. The best-fit N, AGL, and AGV parameters do not produce any significant shoulder at all. It is possible that another form of AG expression, derived from some other temperature dependence for $\Delta C_p(T)$, would better reproduce this feature and still be consistent with the relatively high T_e data presented here.

An approximate Kauzmann analysis of PVC is also possible. Although PVC is thermally unstable and the commercial polymer has very low crystallinity (5–10%), thermal data for highly crystalline PVC have been obtained by Gouinlock.⁵⁰ For 64% syndiotactic (44% crystalline) materials, prepared by two methods, an average melting temperature of 538 K and heat of fusion of 18.8 cal g⁻¹ were determined. Commercial PVC is about 53% syndiotactic, with an estimated melting temperature of about 450 K and entropy of fusion of $0.038 \pm 10\%$ cal K⁻¹ g⁻¹. The value of ΔC_p at T_g is 0.085 cal K⁻¹ g⁻¹,⁵¹ but its temperature dependence is very uncertain because the proximity of broad melting endotherms to T_g ⁵¹ makes an accurate assessment of the liquid heat capacity difficult. We performed Kauzmann analyses assuming both a temperature-independent ΔC_p and an inverse temperature dependence and found $T_2 = 290 \pm 20$ K for each, where the uncertainty corresponds to $\pm 10\%$ in the entropy of melting. The AG values are 320 K (Tables II and III). Given the uncertainties in correcting for syndiotacticity, the breadth of the melting endotherms, and other difficulties in obtaining accurate thermal data for PVC, the AG and Kauzmann values for T_2 are considered to be in satisfactory agreement.

The AG values of T_2 for PVAc, 225 ± 30 K, agree with the value of 238 K obtained by Sasabe and Moynihan³⁸ in their WLF analysis of dielectric relaxation data.

Values of $\Delta\mu$ can readily be estimated from D and $\Delta C_p(T_g)$ in principle, but in practice these depend on the assumed value(s) for s_c^* and on the choice of basic molecular unit (for example, monomer segments or Wunderlich's "beads"). We choose the bead as the fundamental unit and calculate $\Delta\mu$ for $s_c^* = k \ln 2$ and $s_c^* = k \ln 3!$ as reasonable limiting values. The number of beads per monomer segment and values of $\Delta C_p(T_g)$ are taken from a recent review by Mathot.⁵² The results are summarized in Table V. Both sets of $\Delta\mu$ correlate strongly with T_f'/T_2 , with intercepts of $T_f'/T_2 \approx 1$ for $\Delta\mu = 0$ (see below). We note that the datum for PC, which lies off both correlation lines, would shift onto them if s_c^* were increased to the next higher value in the series $k \ln n!$.

The values of $\Delta\mu$ for $s_c^* = k \ln 3!$ are comparable with rotational energy barriers and thus consistent with the AG definition of $\Delta\mu$ as the fundamental energy barrier for configurational rearrangement. There are two possible reasons why the higher value of s_c^* is needed to give this result. One possible explanation may lie in Goldstein's suggestion³³ that there are significant nonconfigurational contributions to $\Delta C_p(T_g)$ (e.g., lattice vibrations, anhar-

monicity, and secondary relaxation effects). This would require that a fraction of order $\ln 2/\ln 3! \approx 0.4$ be configurational, in line with Goldstein's estimates. Another intriguing possibility is the observation by Helfand⁵³ that although a minimum number of three segments is needed for the primary relaxation event in a polymer (a crankshaft motion), the activation energy corresponds to rotation about only one bond. In this case s_c^* may be closer to $k \ln 2^3$, but this is only 16% larger than $k \ln 3!$ and the general consistency of the figures is unaffected. This picture is particularly attractive and suggests that the Adam-Gibbs theory may be close to being quantitatively correct.

We turn now to correlations between D , T_f'/T_2 , and β , a brief discussion of which appeared earlier.⁹ For clarity we focus on the AGV parameters, but since we will be concerned with qualitative trends rather than numerical values the discussion is also valid for AGL. We include the N-derived AGV and β parameters for nonpolymeric materials in our discussion, since we have established above that eq 14 and 15 are good approximations for the polymers, and the best-fit N and AGV values of β for the polymers are in good agreement (Tables I and III). Because the concept of beads in nonpolymeric systems is poorly defined, however, we do not attempt to calculate $\Delta\mu$ for them and restrict our discussion of activation energies to the parameter D .

We begin with D and T_f'/T_2 . Since the present definition of C (eq 12) differs from that given earlier,⁹ the relationships between D , $\Delta\mu$, and Δh^* also differ. Here, we consider the quantity $\Delta\mu s_c^*/\Delta C_p(T_g) \equiv D' = DT_f'/T_2 \approx x^2 \Delta h^*(1-x)^{-1}$ rather than $D = x^2 \Delta h^*$, which has the advantage of eliminating T_2 from the proportionality factor between D' and $\Delta\mu$. A plot of T_f'/T_2 vs. D'/R is given in Figure 13A. As before,⁹ T_f'/T_2 approaches 1.0 as D' decreases to 0.0, consistent with T_f' approaching T_2 as the primary activation energy $\Delta\mu$ decreases to zero. Since $\Delta C_p(T_g)$ and probably s_c^* are material dependent (see above) we attach no significance to the slope, nor to the approximate linearity, of the plot in Figure 13A. However, we repeat our earlier observation that since both $\Delta C_p(T_g)$ and s_c^* are finite and nonzero, the limit $D' \rightarrow 0$ corresponds uniquely to $\Delta\mu \rightarrow 0$. This is confirmed for the polymers, for which $\Delta\mu$ can be explicitly calculated (see above).

The approximately linear relation between D' and T_f'/T_2 corresponds to an approximate proportionality between D' and $1 - T_2/T_f'$ that provides a direct explanation for the inverse correlation between D' (or D) and Δh^* (compare Tables I and III). Equation 13 indicates that Δh^*_{eff} is proportional to D and inversely proportional to $(1 - T_2/T_f')^2 \approx x^2$. Thus as D decreases in approximate proportion to $(1 - T_2/T_f')$, the denominator decreases quadratically and Δh^* increases. The puzzling inverse correlation between x and Δh^* ¹³ is also resolved by the proportionality between D and $1 - T_2/T_f' \approx x$, since $\Delta h^* \approx D/x^2 \approx 1/x$.

Figure 13A shows that the polymers tend to have lower values of D' and T_f'/T_2 . This is apparently unrelated to the strength of intermolecular forces since, for example, the nonpolar 5P4E glass has almost the same parameters as ionic/covalent B_2O_3 , both of which have higher D' and T_f'/T_2 values than polar PVC or PMMA. We speculate that, to the extent that the limited number of materials in Figure 13A are representative of liquids in general, the trend is associated with coordination geometry. Thus inorganic materials such as $NaKS_i_3O_7$ and As_2Se_3 have three-dimensional constraints on configurational rearrangement and larger values of $\Delta\mu$, compared with poly-

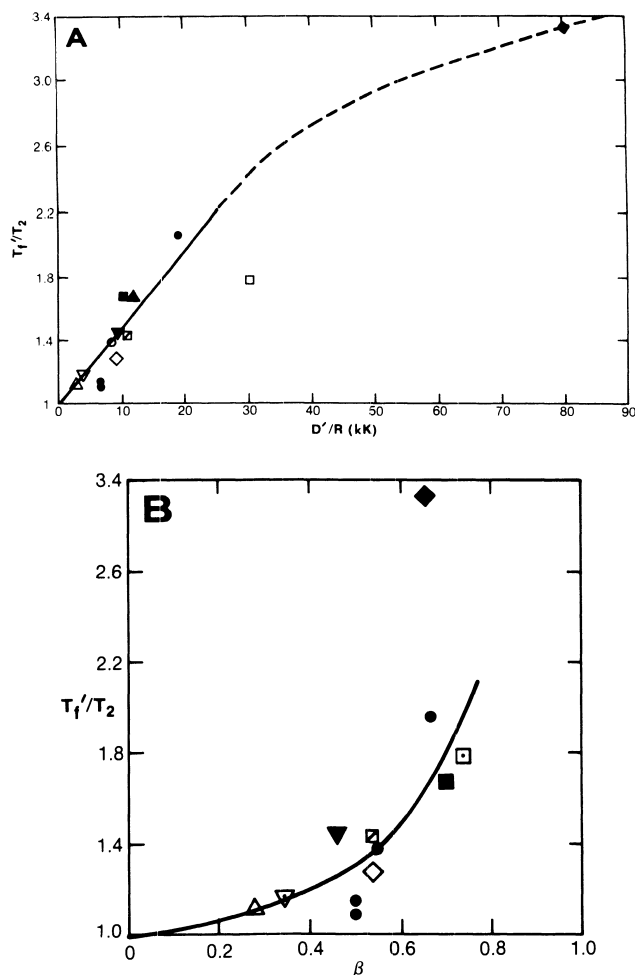


Figure 13. (A) T_f'/T_2 as a function of D'/R , from the AGV parameters given in Table III: PVAc (O); PVC (Δ); PS ($T_2 = 210$ K) (\square); PS ($T_2 = 260$ K) (\square); PMMA (∇); PC (\diamond); As_2Se_3 (\bullet); B_2O_3 (\blacktriangle); 5P4E (\blacksquare); $Ca^{2+}-K^+-NO_3^-$ (\blacktriangledown); $NaKS_i_3O_7$ (\blacklozenge); ZBLA (\bullet). Solid and dashed lines are to aid the eye. (B) T_f'/T_2 as a function of β , from the AGV parameters given in Table III. Solid line is least-squares fit of T_f'/T_2 vs. β^2 (omitting $NaKS_i_3O_7$ datum). Symbols same as in (A).

mers, whose constraints are closer to being one dimensional. This may also account for the similarity of the parameters for ZBLA to those of the polymers,⁴³ if chains of zirconium fluoride polyhedra are assumed to occur in ZBLA glasses. The importance of coordination number and structure has been emphasized by Angell and co-workers^{55,56} and Brawer.¹⁶

A cautionary note must be sounded for these speculations, however. Larger values of T_2 invariably produce smaller values of D in the optimizations, and it is possible that some of the trend apparent in Figure 13A may be attributable to correlated uncertainties in the parameters. A similar effect was noted for the correlation between the N parameters x and Δh^* .¹³

We note in passing that some simple inorganic glasses have unusually low values of T_g/T_2 ,⁵⁵ comparable with those found here for several polymers. These include lithium acetate ($T_g/T_2 \approx 1.1$), $Ca(NO_3)_2 \cdot 4H_2O$ (1.1), and $H_2SO_4 \cdot 3H_2O$ (1.2). Figure 13A suggests that enthalpy relaxation for these materials may be characterized by low values of x (0.1–0.2) and β (0.3–0.4) and high $\Delta h^*/R$ (100–300 kK). Experimental tests of these predictions would be informative.

We suggested earlier⁹ that relaxation might be more cooperative (smaller β) as T_f' approaches T_2 . This is observed (Figure 13B), although the scatter is sizable (linear

Table VI
N Parameters for PS

history ^a	$\Delta h^*/R$, kK	x	β	$\ln A$, s	ϕ	$C_{p,max}^N$	T_f', K
-40/+10	63	0.670	0.656	-164.61	0.057		
	80	0.490	0.658	-211.33	0.020	1.28	375.6
	105	0.377	0.634	-278.13	0.012		
-20/+10	63	0.934	0.598	-165.13	0.051		
	80	0.451	0.687	-211.50	0.016	1.35	373.9
	105	0.509	0.580	-278.85	0.032		
-10/+10	63	0.590	0.768	-164.54	0.012		
	80	0.463	0.694	-211.44	0.032	1.49	372.9
	105	0.344	0.618	-278.36	0.111		
-5/+10	63	0.670	0.823	-164.88	0.013		
	80	0.525	0.718	-211.95	0.027	1.63	371.6
	105	0.396	0.621	-279.10	0.114		
350 K/ 1 h	63	0.600	0.778	-164.57	0.054		
	80	0.462	0.729	-211.40	0.12	1.36	373.4
	105	0.343	0.663	-278.30	0.219		
350 K/ 4 h	63	0.629	0.904	-164.50	0.038		
	80	0.471	0.785	-211.43	0.197	1.82	370.2
	105	0.263	0.536	-277.96	0.333		
350 K/ 16 h	63	0.644	1.000	-164.12	0.267		
	80	0.415	0.648	-211.20	1.00	3.49	368.4
	105	0.262	0.481	-277.78	1.58		
350 K/ 66 h	63	0.653	1.000	-163.31	1.01		
	80	0.459	0.737	-210.39	1.09	5.57	367.5
	105	0.425	0.924	-276.25	10.7		
355 K/ 1 h	63	0.652	0.909	-164.41	1.01		
	80	0.508	0.824	-211.31	0.16	1.70	372.3
	105	0.344	0.681	-278.15	0.342		
360 K/ 1 h	63	0.694	1.000	-164.12	0.084		
	80	0.528	0.840	-211.12	0.41	2.58	370.9
	105	0.304	0.581	-277.85	0.60		
365 K/ 1 h	63	0.748	1.000	-163.55	0.21		
	80	0.599	0.868	-210.48	0.25	3.04	370.7
	105	0.368	0.607	-277.44	0.961		
370 K/ 1 h	63	0.743	0.888	-163.88	0.101		
	80	0.817	0.782	-210.3	0.027	2.17	371.7
	105	0.527	0.544	-277.55	0.186		

^a-QC/+QH or T_e/t_e .

correlation coefficient $r = 0.84$, excluding the anomalous datum for NaKSi_3O_7). A least-squares fit of T_f'/T_2 vs. β^2 gives a comparable fit ($r = 0.86$) and extrapolates to $\beta \approx 0$ at $T_f'/T_2 = 1.0$ (solid line, Figure 13B), suggesting that the average relaxation time ($=\tau_0\Gamma(1/\beta)/\beta$, $\Gamma = \text{gamma}$

function) would become infinite as the number of configurations approached unity at $T_f' = T_2$. The overall decrease in β with T_f'/T_2 appears to be a natural extension of the general observation that β decreases with decreasing temperature above T_g for almost all liquids.

The correlations between T_f'/T_2 , β , and Δh^*_{eff} are all consistent with the classification of liquids above T_g into degrees of "strong" and "fragile" behavior, proposed by Angell.⁵⁵ In this scheme materials that exhibit Arrhenius temperature dependences with small values of Δh^* near T_g , and that tend to have low values of $\Delta C_p(T_g)$ and nearly exponential response functions, are termed "strong". Silica, germania, and beryllium fluoride are examples of strong liquids. "Fragile" liquids, on the other hand, exhibit non-Arrhenius behavior and high effective values of Δh^* near T_g and have large values of $\Delta C_p(T_g)$ and pronounced nonexponential response functions. The liquids of *o*-terphenyl, $0.6\text{KNO}_3-0.4\text{Ca}(\text{NO}_3)_2$, and "ZBLA" (=zirconium, barium, lanthanum, aluminum fluorides) are examples of fragile liquids, which derive their name from a postulated breakdown in structure with increasing temperature. The polymers studied here, with the possible exception of PS, tend to have lower values of T_g/T_2 and to be more non-Arrhenius than the inorganics and are therefore more fragile. Indeed, PVC appears to be the most fragile liquid yet encountered. The polymers also tend to have lower values of β , consistent with their greater fragility. However, the values of ΔC_p for polymers are not particularly large, and there is no correlation between β or T_f'/T_2 and ΔC_p for the polymers as a group, expressed either on a molar or per bead basis, or when normalized by C_{pg} . This is in sharp contrast to the nonpolymeric glasses, which exhibit clear inverse correlations of both β and T_f'/T_2 with $\Delta C_p/C_{pg}$. The distinction is evidently not due to side-chain effects, since PC and PVAc lie on the same correlation line as the nonpolymeric glasses and PVC and PMMA lie far off it. We can offer no explanation for this exceptional behavior of some of the polymers at this time.

"Strong" liquids derive their name from the resistance to thermal degradation of atomic or molecular groupings with well-defined short-range order. Thus the degeneracy of these groupings increases only slightly with temperature, and the configurational heat capacity is small.⁵⁵ However,

Table VII
Best-Fit N Parameters to AGV Generated Data^a

history ^b	$\Delta h^*/R$, kK	x	β	$\ln A$, s	ϕ	$C_{p,max}^N$ (AGV)	T_f' (AGV)
-40/+10	80	0.294	0.488	-221.60	0.009	1.126	372.6
	90	0.228	0.478	-249.18	0.028		
-20/+10	80	0.291	0.487	-221.59	0.0012	1.195	371.5
	90	0.263	0.461	-249.18	0.060		
-10/+10	80	0.291	0.485	-221.59	0.0021	1.294	370.4
	90	0.234	0.454	-249.18	0.065		
-5/+10	80	0.294	0.484	-221.59	0.003	1.464	369.4
	90	0.243	0.444	-249.18	0.111		
350 K/1 h	80	0.333	0.501	-211.37	0.0011	1.143	368.5
	90	0.284	0.480	-238.18	0.0009		
360 K/1 h	80	0.370	0.530	-211.43	0.0069	2.118	367.6
	90	0.291	0.477	-238.18	0.0129		
370 K/1 h	80	0.344	0.515	-211.41	0.0023	2.350	369.5
	90	0.309	0.465	-238.12	0.012		
350 K/4 h	80	0.334	0.490	-211.37	0.012	1.631	366.7
	90	0.297	0.485	-238.24	0.005		
350 K/16 h	80	0.372	0.549	-211.49	0.054	3.58	364.9
	90	0.289	0.463	-238.09	0.033		
350 K/66 h	80	0.393	0.594	-211.27	0.027	10.24	361.7
	90	0.302	0.490	-238.54	0.261		

^a $D/R = 7.85$ kK, $T_2 = 260$ K, $\beta = 0.50$, $\ln A = -65.00$ s. ^b-QC/+QH or T_e/t_e .

such rigid groups would be expected to require a high activation energy for rearrangement, inconsistent with the lower values of Δh^* for strong liquids if Δh^* is interpreted as an activation energy. This difficulty is resolved if $\Delta\mu$ is assumed to be the primary activation energy, because of the inverse relation between $\Delta\mu$ and Δh^* noted above.

Concluding Remarks

From the limited point of view of fitting experimental data, the AGL and AGV formalisms offer only a modest improvement over N for the polymers and thermal histories considered here. However, the AG expressions provide valuable physical insight into relaxation processes in glasses, and enable the empirical N parameters and their correlations to be interpreted in physically significant terms. The N nonlinearly parameter x , for example, is a direct measure of T_f/T_2 , regardless of the specific forms for $\Delta C_p(T)$ and τ_0 . The AG parameter $\Delta\mu$, regarded as a primary activation energy, determines how close T_g can get to T_2 , and therefore determines x as well as Δh^* . The inverse relation between x and Δh^* ¹³ follows directly from the AG-derived relation $\Delta\mu \sim x^2\Delta h^*$. Within broad uncertainties, the AG-derived values of T_2 are also physically reasonable and, in some cases, in reasonable agreement with Kauzmann estimates. Finally, the consistency of the correlations between the AG parameters that describe glassy-state relaxations with the variation in behavior of liquids above T_g strongly suggests that the nonlinearity of glassy-state and glass-transition relaxations is a direct extension of linear relaxation behavior above T_g . The Adam-Gibbs theory, with its natural separation of T and T_f , provides an excellent framework for this extension.

Acknowledgment. I am indebted to G. W. Scherer for stimulating discussions, which inspired the genesis of this work, and have benefitted greatly from discussions with C. T. Moynihan, J. M. O'Reilly, J. Tribone, and C. A. Angell. I thank S. Opalka for providing experimental data for ZBLA.

Registry No. PVAc, 9003-20-7; PVC, 9002-86-2; PS, 9003-53-6; PMMA, 9011-14-7; PC (homopolymer), 25037-45-0; PC (SRU), 24936-68-3.

References and Notes

- (1) Goldstein, M. In *Modern Aspects of the Vitreous State*; MacKenzie, J. P., Ed.; Butterworths: London, 1964; Vol. 3, pp 90-125.
- (2) Ritland, H. N. *J. Am. Ceram. Soc.* **1956**, *39*, 403.
- (3) Kovacs, A. J. *Fortschr. Hochpolym.-Forsch.* **1963**, *3*, 394.
- (4) Tool, A. Q. *J. Am. Ceram. Soc.* **1946**, *29*, 240.
- (5) Tool, A. Q.; Eichlin, C. G. *J. Am. Ceram. Soc.* **1931**, *14*, 276.
- (6) Narayanaswamy, O. S. *J. Am. Ceram. Soc.* **1971**, *54*, 491.
- (7) Mazurin, O. V.; Rekhson, S. M.; Startsev, Yu. K. *Fiz. Khim. Stekla* **1975**, *1*, 438.
- (8) Moynihan, C. T.; Easteal, A. J.; DeBolt, M. A.; Tucker, J. J. *Am. Ceram. Soc.* **1976**, *59*, 12.
- (9) Hodge, I. M. *Macromolecules* **1986**, *19*, 936.
- (10) Vogel, H. *Phys. Z.* **1921**, *22*, 645.
- (11) Williams, M. L.; Landel, R. F.; Ferry, J. D. *J. Am. Chem. Soc.* **1955**, *77*, 3701.
- (12) Hodge, I. M.; Berens, A. R. *Macromolecules* **1982**, *15*, 762.
- (13) Hodge, I. M. *Macromolecules* **1983**, *16*, 898.
- (14) Prest, W. M., Jr.; Roberts, F. J., Jr.; Hodge, I. M. In *Proceedings of the 12th NATAS Conference*, Sept 1980, Williamsburg, VA; pp 119-123.
- (15) Tribone, J. T.; O'Reilly, J. M.; Greener, J. *Macromolecules* **1986**, *19*, 1732.
- (16) Brawer, S. *Relaxation in Viscous Liquids and Glasses*; American Ceramic Society: Columbus, OH, 1985.
- (17) Chen, H. S.; Kurkjian, C. R. *J. Am. Ceram. Soc.* **1983**, *66*, 613.
- (18) Macedo, P. B.; Litovitz, T. A. *J. Chem. Phys.* **1965**, *62*, 245.
- (19) Dienes, G. J. *J. Appl. Phys.* **1953**, *24*, 779.
- (20) Mazurin, O. V.; Kluyev, V. P.; Stolyar, S. V. *Glastech. Ber.* **1983**, *56*, 1148.
- (21) Adam, G.; Gibbs, J. H. *J. Chem. Phys.* **1965**, *43*, 139.
- (22) Gibbs, J. H.; DiMarzio, E. A. *J. Chem. Phys.* **1958**, *28*, 373.
- (23) Plazek, D. J.; Magill, J. H. *J. Chem. Phys.* **1966**, *45*, 3038.
- (24) Magill, J. H. *J. Chem. Phys.* **1967**, *47*, 2802.
- (25) Hodge, I. M. *Bull. Am. Phys. Soc.* **1985**, *30*, 584.
- (26) Howell, F. S.; Bose, P. A.; Macedo, P. B.; Moynihan, C. T. *J. Phys. Chem.* **1974**, *78*, 639.
- (27) Matsuoka, S. *J. Rheol.* **1986**, *30*, 869.
- (28) Scherer, G. W. *J. Am. Ceram. Soc.* **1984**, *67*, 504.
- (29) Napolitano, A.; Simmons, J. H.; Blackburn, D. H.; Chichester, R. E. *J. Res. Natl. Bur. Stand., Sect. A* **1974**, *78A*, 323.
- (30) DeBolt, M. A. Ph.D. Thesis, Catholic University of America, 1976.
- (31) Sasabe, H.; DeBolt, M. A.; Macedo, P. B.; Moynihan, C. T. *Proceedings of the 11th International Congress on Glass*; Prague, 1977.
- (32) Kauzmann, W. *Chem. Rev.* **1948**, *43*, 219.
- (33) Goldstein, M. *J. Chem. Phys.* **1976**, *64*, 4767.
- (34) Miller, A. A. *Macromolecules* **1978**, *11*, 859.
- (35) Gujrati, P. D.; Goldstein, M. *J. Chem. Phys.* **1981**, *74*, 2596.
- (36) Rekhson, S. M.; Bulaeva, A. V.; Mazurin, O. V. *Izv. Akad. Nauk. SSSR, Neorg. Mat.* **1971**, *7*, 714.
- (37) Hodge, I. M.; Huvar, G. S. *Macromolecules* **1983**, *16*, 371.
- (38) Sasabe, H.; Moynihan, C. T. *J. Polym. Sci.* **1978**, *16*, 1667.
- (39) Moynihan, C. T.; Macedo, P. B.; Montrose, C. J.; Gupta, P. K.; DeBolt, M. A.; Dill, J. F.; Dom, B. E.; Drake, P. W.; Easteal, A. J.; Elterman, P. B.; Moeller, R. P.; Sasabe, H.; Wilder, J. A. *Ann. N.Y. Acad. Sci.* **1976**, *279*, 15.
- (40) DeBolt, M. A.; Easteal, A. J.; Macedo, P. B.; Moynihan, C. T. *J. Am. Ceram. Soc.* **1976**, *59*, 16.
- (41) Moynihan, C. T.; Sasabe, H.; Tucker, J. *Proceedings of the International Symposium on Molten Salts*; Electrochemical Society: Pennington, NJ, 1976; p 182.
- (42) Moynihan, C. T.; Easteal, A. J.; Tran, D. C.; Wilder, J. A.; Donovan, E. P. *J. Am. Ceram. Soc.* **1976**, *53*, 137.
- (43) Moynihan, C. T.; Bruce, A. J.; Gavin, D. L.; Loehr, S. R.; Opalka, S. M.; Drexhage, M. G. *Polym. Eng. Sci.* **1984**, *24*, 1117.
- (44) Privalko, V. P.; Demchenko, S. S.; Lipatov, Y. S. *Macromolecules* **1986**, *19*, 901.
- (45) Ngai, K. L. *Comments Solid State Phys.* **1979**, *9*, 127.
- (46) Rendell, R. W.; Ngai, K. L. In *Relaxations in Complex Systems*; Ngai, K. L., Wright, G. B., Eds.; Office Naval Research: Washington, DC, 1984; p 309.
- (47) Karasz, F. E.; Bair, H. E.; O'Reilly, J. M. *J. Phys. Chem.* **1965**, *69*, 2657.
- (48) Miller, A. A. *Macromolecules* **1970**, *3*, 674.
- (49) Chen, H. S.; Wang, T. T. *J. Appl. Phys.* **1981**, *52*, 5898.
- (50) Gouinlock, E. V. *J. Polym. Sci., Polym. Phys.* **1975**, *13*, 1533.
- (51) Lehr, M. H.; Parker, R. G.; Komoroski, R. A. *Macromolecules* **1985**, *18*, 1265.
- (52) Mathot, V. B. F. *Polymer* **1984**, *25*, 579.
- (53) Helfand, E. *Science (Washington, D.C.)* **1984**, *226*, 647.
- (54) Angell, C. A.; Hodge, I. M.; Cheeseman, P. A. *Proceedings of the International Symposium on Molten Salts*; Electrochemical Society: Pennington, NJ, 1976; p 138.
- (55) Angell, C. A. In *Relaxations in Complex Systems*; Ngai, K. L., Wright, G. B., Eds.; Office of Naval Research: Washington, DC, 1984; p 3.
- (56)